

Immunofluorescence Microscopy of Organized Microtubule Arrays in Structurally Stabilized Meristematic Plant Cells

SUSAN M. WICK, ROBERT W. SEAGULL, MARY OSBORN, KLAUS WEBER, and BRIAN E. S. GUNNING

Department of Developmental Biology, Research School of Biological Sciences, The Australian National University, Canberra, A. C. T. 2601, Australia, and the Max Planck Institute for Biophysical Chemistry, D-3400 Göttingen, Federal Republic of Germany

ABSTRACT Cells were prepared for indirect immunofluorescence microscopy after paraformaldehyde fixation of multicellular root apices and brief incubation in cell wall-digesting enzymes. This allowed subsequent separation of the tissue into individual cells or short files of cells which were put onto coverslips coated with polylysine. Unlike spherical protoplasts made from living tissues, these preparations retain the same polyhedral shape as the cells from which they are derived. Cellular contents, including organized arrays of microtubules, are likewise structurally stabilized. Antibodies to porcine brain tubulin react with all types of microtubule array known to occur in plant meristematic cells, namely, interphase cortical microtubules, pre-prophase bands, the mitotic spindle, and phragmoplast microtubules.

The retention of antigenicity in permeabilized, isolated, stabilized cells from typical, wall-enclosed plant cells has much potential for plant immunocytochemistry, and in particular should facilitate work on the role of microtubules in the morphogenesis of organized plant tissues.

Microtubules participate as morphogenetic tools in two basic processes by which plants develop their characteristic forms: (a) production of new cells in specific sites and with specific initial shapes by partitioning of parental cells, and (b) further shaping of the progeny during their expansion and differentiation (8, 18). In respect of (a), microtubules are present in the mitotic spindle, where they develop in the absence of centrioles (14). Immediately before the division cycle they are deposited as a transitory "pre-prophase band" (PPB) (8, 26, 27), which in its positioning predicts the site and plane of the future cytokinesis. At telophase another microtubule system contributes to the organization of the phragmoplast, which contains the new partitioning wall, or cell plate. In respect of (b), there are many instances of congruence between the orientation of microtubules in the cell cortex during interphase ("interphase cortical arrays") and the orientation of currently deposited microfibrils of cell wall material (see 12 and 15 for recent summaries). The inference is that the cell exerts geometrical control over its expansion by setting up specifically oriented microtubule arrays. These in turn guide wall deposition, thereby regulating the mechanical properties of the wall and determining its spatial reaction to the turgor forces that drive cell expansion.

Until recently, the only available method for studying the various categories of microtubule array was electron microscopy. However, to gain detailed information on three-dimensional relationships from ultrathin sections, recourse to time-consuming serial sectioning (12, 13) and high-voltage electron

microscopy (7) has proved necessary. Immunofluorescence methods, so successfully applied to the study of cytoskeletal components of animal tissue culture cells (2, 30), would be an ideal alternative to electron microscopy for visualizing overall organization of plant cell microtubules, but the wall that encloses the typical plant cell has proved to be a severe obstacle (20). This complex of polysaccharide and protein has a pore size of 3–5 nm (3), and thus impedes the passage of antibodies. Accordingly, previous use of tubulin immunofluorescence techniques on plants took advantage of highly specialized cells or preparations, namely, naked algal gametes (31); liquid endosperm cells (5, 6), which are droplets of wall-less protoplasm bounded by a membrane; protoplasts derived from algae, moss protonema, and higher plant cells grown in suspension culture, the antibodies being applied either to the intact protoplasts (22, 23, 28) or to plasmalemma fragments left after osmotic bursting (24, 29); and "partial protoplasts" made by enzymatically removing part of the wall from living suspension culture cells (22, 23).

While demonstrating that plant and animal tubulins are antigenically similar, the above preparations have disadvantages. When protoplasts are formed, cells round up and lose the three-dimensional spatial characteristics they possessed *in vivo*. The majority of microtubules found in protoplasts are randomly oriented (29), unlike the highly aligned arrays seen by electron microscopy in typical cells within an organized tissue (8, 13). The patterns of fluorescence in partial protoplasts

from suspension culture cells no doubt represent *in vivo* arrays of microtubules but in these single cells the cellular interactions that determine the form of tissues and organs are lacking. Also to date there has been no way to examine with immunofluorescence the PPB of microtubules. This array is found in cells of multicellular tissues and is postulated to be involved in positioning the new cell wall at the subsequent cytokinesis (26, 27). It is therefore morphogenetically important in the plant, but is not found in suspension culture cells (4) or in liquid endosperm cells (1).

Clearly, a method that preserves tubulin-antibody reactivity and permits application of immunofluorescence procedures to cells that retain *in vivo* spatial properties would open the way to many studies of the cytoskeleton and its role in plant development. In the present paper we report progress in this direction.

MATERIALS AND METHODS

Cell Preparations

Seeds of onion (*Allium cepa* L.) were germinated in the dark at room temperature on filter paper moistened with distilled water. When the roots were at least 1 cm long, the apical 1–4 mm was cut off and fixed for 1 h in freshly prepared 3.7% paraformaldehyde either in phosphate-buffered saline (PBS), pH 7.4, or in 50 mM potassium phosphate buffer, pH 6.8. Root tips were then rinsed with buffer for at least 30 min and exposed to one of the following wall-digesting enzymes, each dissolved in 0.4 M mannitol: (a) 0.5% cellulase (Onozuka R-10; Kinki Yakult, Nishinomiya, Japan) for 20–25 min; (b) 2% driselase (Kyowa-Hakko-Kogyo, Tokyo, Japan) (filtered) for 12–15 min; (c) 1% cellulysin (Calbiochem-Behring Corp., American Hoechst Corp., San Diego, Calif.) for 13–16 min.

After another buffer rinse, root tips were squashed between coverslips to release individual cells. The coverslips were first cleaned in acetone, exposed to a freshly prepared 1 mg/ml solution of poly-L-lysine for at least 1 h, drained, rinsed with distilled water, and air-dried immediately before use. When root tips were sufficiently squashed, as determined by phase microscopy, the cover slips were separated, large fragments of root were removed, and the cell suspensions were allowed to settle. Some preparations were allowed to air dry to maximize attachment. Cells and debris not adhering were removed by a buffer rinse. Coverslips carrying the isolated cells were then plunged into prechilled methanol, -10°C , for 6–8 min to make membranes permeable to antibodies, and rehydrated in PBS. The effects of a 20- to 30-min detergent extraction in microtubule-stabilizing buffer, performed at room temperature before or after the organic solvent step, were investigated. This solution consisted of 1% Triton X-100, 0.1 M PIPES, 2 mM EGTA, 1 mM MgSO_4 , and 0.4 M mannitol, pH 6.9. The possibility that EGTA might enhance microtubule preservation and facilitate cell separation was also explored. For some preparations, 5 mM EGTA was included either in the fixative alone or in all solutions from fixation through the cold methanol step.

Once cells were attached to coverslips, they were processed according to standard techniques for indirect immunofluorescence (32).

Cells fixed, digested, and squashed as above were examined with Nomarski optics to assay for structural preservation, as were cells fixed in glutaraldehyde/EGTA and subjected to driselase/EGTA for 2–16 h. Other roots, fixed and digested as for immunofluorescence, were refixed in glutaraldehyde and OsO_4 , embedded without squashing, and sectioned for electron microscopy.

Antibodies

The tubulin antibody, which was raised in rabbits against purified pig brain tubulin and made monospecific by affinity column chromatography, has been described and its specificity documented (25, 32). It was used at a final dilution of 50 μg IgG/ml in PBS. The second antibody was goat anti-rabbit IgG, labeled with fluorescein (Miles-Yeda, Israel) diluted 1:24 with PBS. Controls included use of several normal rabbit sera, which gave no staining of the tubulin-containing structures when used at a 1:10 dilution.

Microscopy

Fluorescence observations were made with a Zeiss photomicroscope using epifluorescence and standard fluorescein filters, and photographed on Kodak Tri-X film. Because of the three-dimensional nature of the microtubule arrays,

most pictures were taken with a $\times 40$ planapo oil immersion objective lens, NA = 1.0, to take advantage of the balance between relatively large depth of field and high fluorescence intensity obtained with that lens. For focusing on surfaces of arrays, it was sometimes possible to use a $\times 63$ planapo lens, NA = 1.4. Phase microscopy was used to verify cell cycle stages represented by the fluorescence images.

Ultrathin sections were examined with a Hitachi H-500 electron microscope.

RESULTS

Isolation of Cells

Isolated cells were obtained with each of the three enzyme treatments. Yield and structural integrity of cells depended on the enzyme, length of digestion, whether EGTA had been used, and on the force applied while squashing roots. Digestion times longer than those given in Materials and Methods caused cytoplasmic damage in formaldehyde-fixed cells. However, a short incubation with wall-digesting enzymes did not alter general ultrastructure, and microtubules were normal in appearance and orientation as assessed by electron microscopy (Fig. 1), as they were in glutaraldehyde-fixed material even after overnight digestion in driselase.

Driselase digestion will yield wall-less cells (giving no fluorescence with Calcofluor M2R new) after fixation with glutaraldehyde. The treatment with wall-digesting enzymes used here, necessarily short for the sake of structural preservation, did not remove or markedly alter cell walls, as judged by electron microscopy of embedded roots. Nevertheless, antibodies penetrated the cells. In the absence of EGTA, considerable squashing pressure was needed to separate the cells. Many ruptured cells and free nuclei were found after driselase digestion and to a lesser extent with cellulysin. Inclusion of EGTA in the fixative did not have a noticeable effect on microtubule preservation, but made possible the isolation of

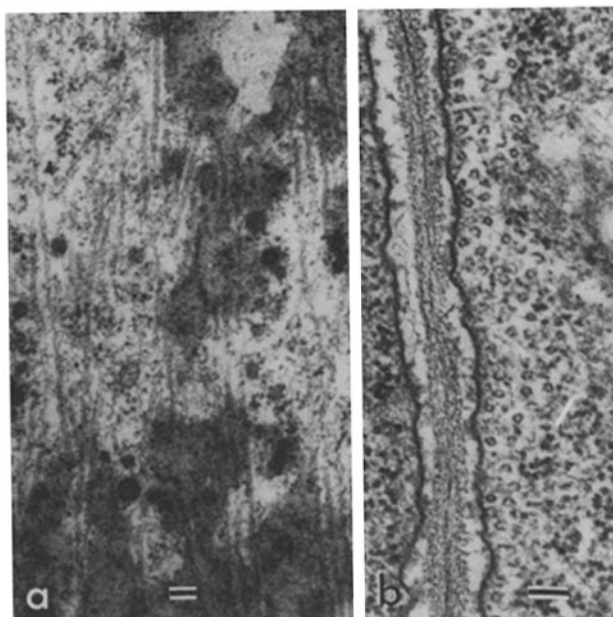


FIGURE 1 Ultrathin sections to show that microtubules survive in cells of *Allium* root tips fixed in formaldehyde/EGTA, subsequently digested for 15 min in driselase/EGTA, and re-fixed in glutaraldehyde. (a) Grazing section through plasmalemma and cortical cytoplasm that contains interphase microtubules. (b) Cross section of a PPB of microtubules. The cytoplasm is very similar to that processed according to standard procedures. Bars, 0.1 μm . (a) $\times 36,000$. (b) $\times 54,000$.

undamaged cells from roots incubated with any of the enzymes. This is presumably a result of partial dissolution, by means of Ca^{++} chelation, of middle lamella Ca^{++} pectates that "cement" adjacent cell walls together (19, 21). Weakening of intercellular bonding was enhanced when EGTA was included in buffer rinses as well as in the fixative and enzyme solutions, yielding cells such as seen in Fig. 2. Many wall fragments and other cellular debris released by the squashing were visible with phase-contrast or Nomarski optics, especially in preparations that had been air-dried onto the polylysine surface. However, these rarely interfered with the fluorescence microscopy, and the increased cell density on the air-dried coverslips was highly desirable.

Detergent extraction of isolated cells did not alter the immunofluorescence patterns, and was not routinely used.

Tubulin Immunofluorescence Patterns

Microtubule arrays were visualized throughout all stages of the cell cycle of *Allium* root tip cells. Interphase cortical arrays are easily discerned on patches of plasmalemma that remain attached to the polylysine when the shear forces of squashing and coverslip separation tear away the rest of the cell (Fig. 3a). Unlike plasmalemma fragments from burst algal (24) or higher plant (29) protoplasts, which show randomly arranged microtubules, these patches illustrate the aligned cortical microtubule orientation in polarized cells from organized tissues (8, 13). While the thickness of an intact cell can make resolution of individual microtubules or small microtubule bundles difficult, their circumferential orientation is still clearly visible (Fig. 3b-d), as reported also by Lloyd et al. (22, 23). In Fig. 3d, several of the fluorescent fibers can be traced as they go around the cell corners, following the polyhedral cell outline.

Cells isolated according to our procedures have provided the

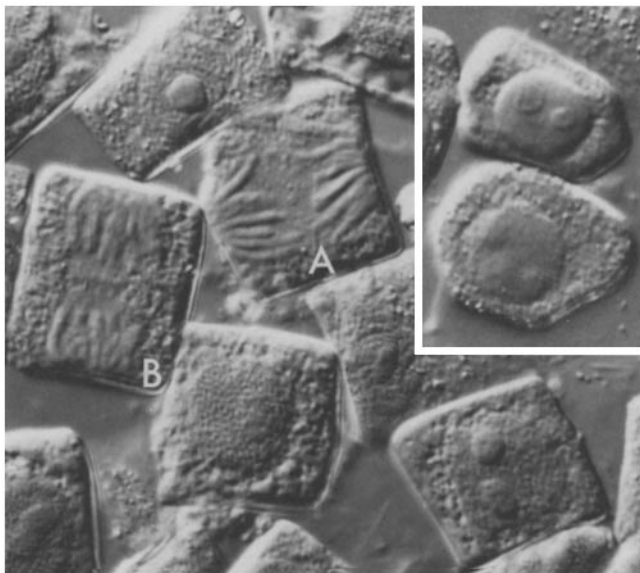
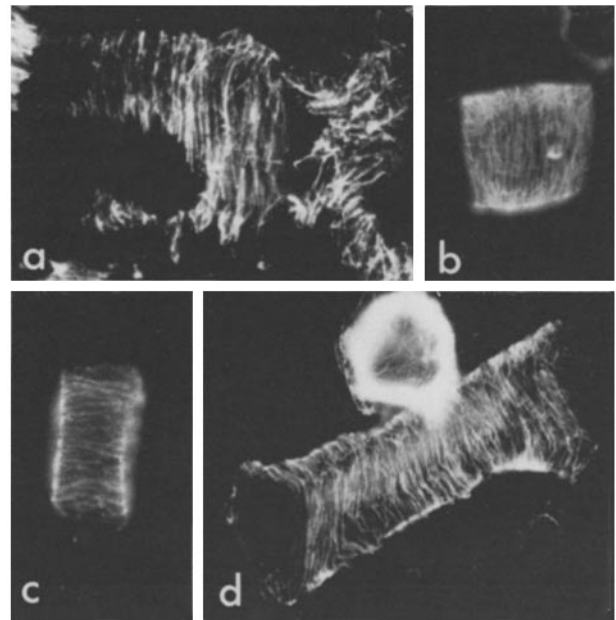


FIGURE 2 Nomarski view of cells from a root fixed in glutaraldehyde/EGTA and digested for 2 h in driselase/EGTA. Cells have maintained the same shapes that they had in the intact tissue. Cell A is in late anaphase. Cell B is in telophase-cytokinesis; the phragmoplast extends for about one-third of the width of the cell. Inset: Cells fixed in paraformaldehyde/EGTA and digested for 20 min in cellulase/EGTA, to show that the procedures used before antibody application also preserve original polyhedral cell shapes and internal structures. $\times 290$. Inset, $\times 320$.



FIGURES 3-5 Indirect immunofluorescence microscopy using antibodies to tubulin.

FIGURE 3 (a-d) Interphase. Cortical microtubules are associated with plasmalemma fragments that remain on the coverslip when the rest of cell is sheared away (a). In intact cells, also, the parallel orientation of interphase arrays is apparent, and individual fluorescent fibers can be followed across the face (b-d) and even around the corners (d) of polyhedral cells. The bright polygonal object at the top in d is an end-on view of a cell showing cumulative fluorescence of cortical microtubules through the length of the cell, the sparse randomly oriented microtubules in the center being those of the cell cortex underlying an end wall. (a) $\times 1,000$. (b) $\times 750$. (c) $\times 880$. (d) $\times 640$.

first opportunity for immunofluorescence study of the PPB. Microtubules of the PPB run circumferentially around the cell cortex (26, 27). Therefore, a view of any side of a cell with a transverse PPB is normal to the plane of the PPB. Cell thickness is such that one can focus on the near or far surface of the band (Fig. 4a, c, and e) or on a median plane (Fig. 4b and d). Not only does the PPB itself fluoresce intensely, but often there is fluorescence associated with the nuclear envelope (Fig. 4a, c-e). Whether this represents microtubules or a nonpolymerized, membrane-bound form of tubulin, or both, is not certain, but some images indicate the presence of fibrous elements that have reacted with the antibodies (Fig. 4c and e). Microtubules lying along or near the nuclear envelope during pre-prophase have been noted (27), although in the closely related species *Allium sativum* they are not seen near the nucleus until prophase, when the PPB has already disappeared (11). It is of interest that when cells are broken, free nuclei still girdled by PPB can be obtained (Fig. 4d and e).

The tubulin immunofluorescence pictures of mitosis in isolated *Allium* cells and those in *Leucospermum* endosperm show many similarities (5, 6). In addition to the reaction with spindle fibers (Fig. 5a-m), a diffuse staining of the polar cap, into which the microtubules insert, is evident (Fig. 5a-d, g, h, and j). *Allium* root tip cells are much smaller than endosperm cells, and some details are consequently harder to see. However, individual fibers can readily be traced. At prophase, it is possible to follow individual fluorescent fibers for nearly the entire pole-to-pole distance (Fig. 5a-c). Focusing through a

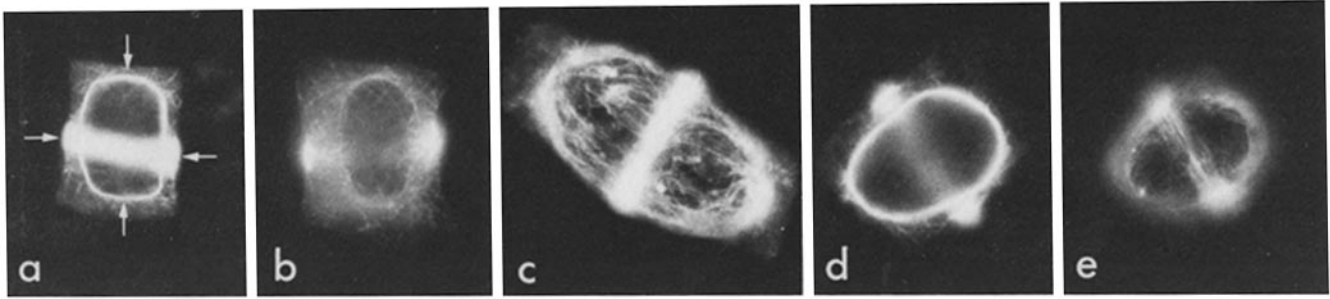


FIGURE 4 (a–e) Pre-prophase. The circumferential PPB (horizontal arrows) is viewed edge-on in all figures (i.e., the plane of the PPB is normal to that of the page). *a–c* are whole cells. In *a*, in addition to intense PPB fluorescence, the nuclear envelope (vertical arrows) is clearly outlined. *b* is focused on cytoplasmic microtubules that are not part of the PPB. Cumulative fluorescence of PPB microtubules oriented perpendicular to the page along the cell's side walls produces the typical edge effect when neither upper nor lower surface of the PPB is in focus. The plane of focus in *c* includes the PPB and the surface of the nuclear envelope, which appears to have associated microtubules as well as diffuse polar fluorescence. *d* and *e* are two levels of focus of the same nucleus: *d* is a median view that emphasizes the nuclear envelope and the edge effect of the PPB; *e* is a view of the upper surface of the PPB where some of the individual microtubules or small bundles of microtubules of this parallel array can be discerned. (*a*) $\times 770$. (*b*) $\times 800$. (*c*) $\times 1,150$. (*d*) $\times 820$. (*e*) $\times 820$.

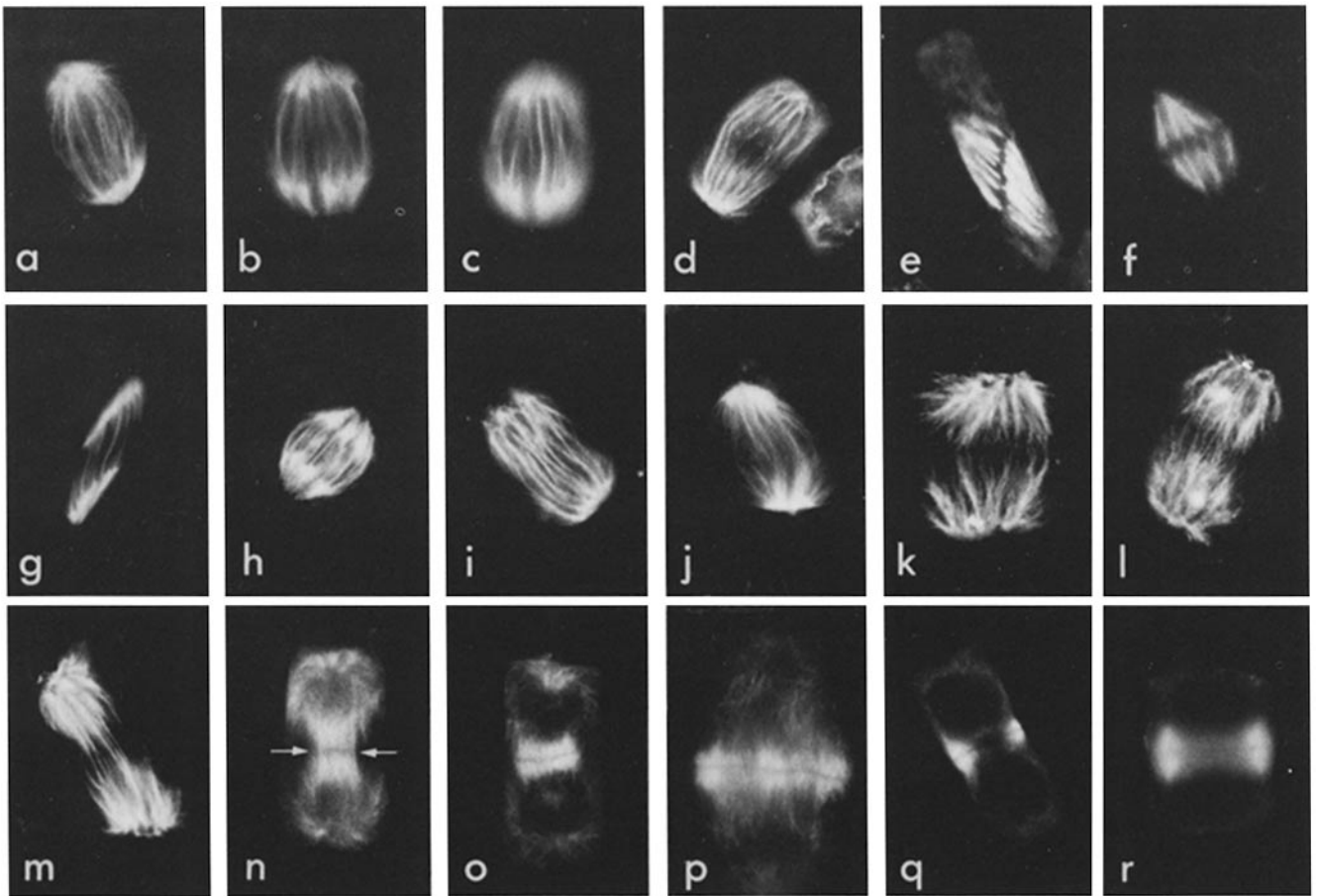


FIGURE 5 (a–m) Mitosis. Prophase, *a–c*. Polar microtubules form a fluorescent “cage” around the nucleus. Views *b* and *c* are different levels of focus of the cell shown in Fig. 6 *a*. Prometaphase, *d*. Metaphase, *e* and *f*; *e* corresponds to Fig. 6 *b*; *f* is an isolated mitotic apparatus. Anaphase, *g–m*. *g* corresponds to Fig. 6 *c* and *d*; an isolated early anaphase spindle is seen in *h*. Mid-anaphase cells, *i–k*; late anaphase, *l* and *m*. (*a*) $\times 850$. (*b*) $\times 850$. (*c*) $\times 850$. (*d*) $\times 850$. (*e*) $\times 620$. (*f*) $\times 640$. (*g*) $\times 480$. (*h*) $\times 640$. (*i*) $\times 800$. (*j*) $\times 720$. (*k*) $\times 770$. (*l*) $\times 800$. (*m*) $\times 660$. (*n–r*) Cytokinesis. Fluorescence patterns of cells in early cytokinesis reveal the remnants of spindle microtubules in polar areas, as well as the large numbers of microtubules in the phragmoplast (between arrows) (*n*, same cell as in Fig. 6 *e*). By the time the phragmoplast has expanded circumferentially nearly all the way to the side walls, its microtubules are shorter and polar fluorescence has decreased (*o*). The isolated phragmoplast (*p*) allows resolution of some of the individual microtubules in the dense ring that circumscribes the new cell plate. At the end of cytokinesis, when the few remaining microtubules are at the cell periphery, they are seen as a small intense patch when the microscope is focused medially within the cell (*q*, same cell as in Fig. 6 *f*) or as a fluorescent “halo” when focused near the surface (*r*). (*n*) $\times 880$. (*o*) $\times 770$. (*p*) $\times 950$. (*q*) $\times 800$. (*r*) $\times 1,000$.

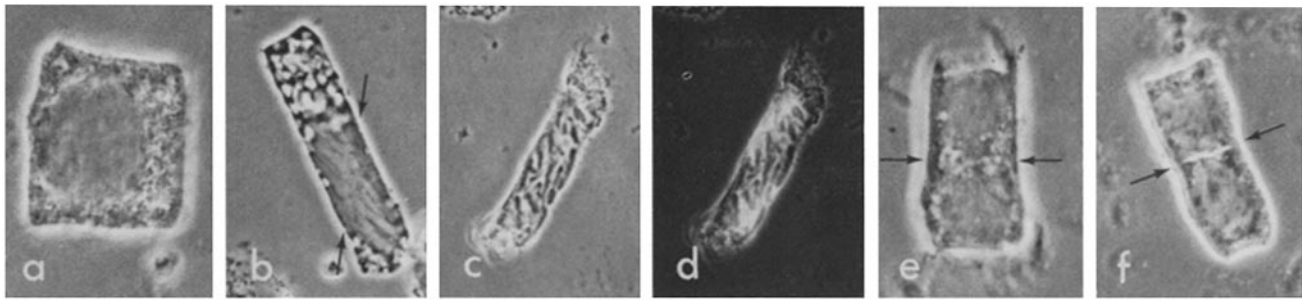


FIGURE 6 Phase-contrast view of some of the cells of Fig. 5. 6 *a* corresponds to 5 *b* and *c*, prophase; 6 *b* to 5 *e*, metaphase; 6 *c* to 5 *g*, anaphase; 6 *e* to 5 *n* cytokinesis; 6 *f* to 5 *q*, end of cytokinesis. 6 *d* is a combined fluorescence and phase view of cell in Figs. 5 *g* and 6 *c*. (a) $\times 850$. (b) $\times 620$. (c) $\times 480$. (d) $\times 480$. (e) $\times 860$. (f) $\times 800$. Arrows in *b*, *e*, and *f* indicate plane of metaphase plate, phragmoplast, and cell plate, respectively.

cell reveals the three-dimensional aspect of this array of non-kinetochore or polar microtubules (Fig. 5 *b* and *c*). Comparison with the corresponding phase-contrast view (Fig. 6 *a*), printed at the same magnification, indicates that the fluorescent fibers lie outside the nucleus and that the diffuse polar fluorescence extends from the nuclear envelope toward the ends of the cell.

At prometaphase and metaphase, kinetochore fibers extend from the poles toward the chromosomes congregating at the metaphase plate (Fig. 5 *d-f*). The chromosomes do not react with antitubulin and are therefore invisible in the fluorescence mode, but their disposition is seen in phase contrast (Fig. 6). Thus, in Fig. 6 *b* (same cell as in Fig. 5 *e*), metaphase kinetochores are aligned diagonally relative to the cell axes, in the same plane in which fluorescent fibers (presumed to be kinetochore fibers) terminate. The half-spindles move apart as anaphase progresses and, with focusing, both the polar and kinetochore fibers and the diffuse fluorescence of the polar cap are visible (Fig. 5 *g-m*). The phase picture (Fig. 6 *c*) and combined phase-fluorescence picture (Fig. 6 *d*) of the anaphase cell of Fig. 5 *g* show kinetochores pointing towards the poles of the mitotic apparatus, which in this case also is diagonal to the long axis of the cell. The diagonal spindles of Fig. 5 *e*, *g*, and *j* possibly represent divisions in which the new cell plate is to be laid down longitudinally with respect to the parent cell, but in which the narrowness of those cells does not allow the spindle to be established or chromosomes to be separated transversely.

The transition from mitosis to cytokinesis is marked by the appearance of phragmoplast microtubules in the mid-zone between separating daughter nuclei at late anaphase (Fig. 5 *l* and *m*). In the micrographs included here, the phragmoplast is seen in edge view (i.e., the plane of the phragmoplast is perpendicular to that of the page), and its microtubules lie perpendicular to and at the edge of the expanding new cell plate (see also 16 and 17). Viewed thus, the near and far edges of a young phragmoplast are close together, and the microtubular fluorescence at any level of focus within it is intense (Fig. 5 *n*). The corresponding phase picture shows the daughter nuclei and accumulating cell plate material (Fig. 6 *e*). As the phragmoplast grows it becomes possible to focus near the central plane of the cell plate (Fig. 5 *q*) or nearer to one of the edges (Fig. 5 *o*, *p*, and *r*), in which case individual fibrous elements can be seen (Fig. 5 *p*). As cytokinesis nears completion, the expanding cell plate appears bright in phase contrast (Fig. 6 *f*, same cell as in Fig. 5 *q*). Phragmoplast microtubules then remain only in the narrow gap between the edges of the plate and the parental walls (Fig. 5 *q* and *r*).

DISCUSSION

With most higher plant material, successful application of

immunofluorescence techniques requires a means of isolating structurally stabilized cells from multicellular tissues and a means of allowing ingress of antibody molecules. Our approach to meeting these requirements has been (a) to fix root tips in paraformaldehyde in an attempt to optimize the balance between cellular (especially microtubular) preservation and preservation of tubulin antigenicity, (b) to break the integrity of the cell wall and cellular co-adhesion with a short incubation in wall-digesting enzymes, (c) to separate cells by squashing the roots and, finally, (d) to permeabilize the plasmalemma with cold methanol. In spite of the brevity of the enzyme treatment, this and the subsequent squashing are capable of weakening or perforating the cell wall sufficiently to allow it to pass antibody molecules. As reported earlier by others using much higher concentrations and longer exposures to another Ca^{++} chelator, EDTA (19, 21), inclusion of 5 mM EGTA in all processing steps appears to aid in the cell separation, and results in a higher proportion of intact, undistorted cells after the squashing. Permeabilized, isolated, stabilized plant cells obtained in this way react with affinity-purified antibodies to porcine brain tubulin to reveal microtubule arrays throughout all stages of the cell cycle. Mitotic spindles, PPBs, phragmoplasts, and cortical arrays are clearly visible. Where microtubule density is low enough, thin fluorescent fibers, almost certainly individual microtubules, can be traced, as in the case of well-spread cultured animal cells (2).

We have successfully applied the techniques described here to root tips of *Zea*, *Brachycome*, and *Azolla*, in addition to *Allium*. The *Azolla* meristem is especially interesting morphogenetically, because division planes are predictable, there are many asymmetrical divisions (10), and with gentle squashing it is possible to obtain files of several permeabilized cells which thus retain their spatial interrelationships. Tubulin antibodies promise to be particularly advantageous in experiments on relationships between the PPB, the subsequent plane of cell division, and the location and behavior of cortical microtubule-initiating sites, which, except in *Azolla* (7, 9), have rarely been detected in higher plants. Characterization of the normal microtubule patterns and of microtubule-initiating site distribution using immunofluorescence techniques should provide a firm foundation for comparisons with tissues that have been induced to undergo abnormal morphogenesis by exposure to a pulse of a microtubule poison or an inhibitor of cytokinesis.

The most appealing feature of the immunofluorescence procedure is its capacity to provide three-dimensional views. This is especially important for studies of plant cells, in which cell thickness makes it difficult to ascertain the overall organization of microtubules using electron microscopy. For instance, the PPB, which is critical in determination of the future plane of

division, has never previously been visualized in its entirety. The images obtained here show symmetrically and asymmetrically placed PBBs as well as those of different orientations relative to the longitudinal axis of the cell. With the aid of appropriate inhibitors, we should be able to investigate the factors that control positioning of the PPB. We have also undertaken a study of the mode and timing of development of the band in *Allium* by means of cell cycle analysis in conjunction with immunofluorescence.

We thank our colleagues at the Max Planck Institute, the Australian National University, and the University of Massachusetts, Amherst, for their help. Cellulase was the generous gift of Dr. D. G. Robinson, University of Göttingen.

Received for publication 12 January 1981, and in revised form 9 March 1981.

REFERENCES

- Bajer, A., and J. Mole-Bajer. 1971. Architecture and function of the mitotic spindle. *Adv. Cell Mol. Biol.* 1:213-266.
- Brinkley, B. R., S. H. Fisel, J. M. Marcum, and R. L. Pardue. 1980. Microtubules in cultured cells—indirect immunofluorescent staining with tubulin antibody. *Int. Rev. Cytol.* 63:59-96.
- Carpita, N., D. Sabularse, D. Montezinos, and D. P. Delmer. 1979. Determination of the pore size of cell walls of living plant cells. *Science (Wash. D. C.)*. 205:1144-1147.
- Fowke, L. C., and O. L. Gamborg. 1980. Applications of protoplasts to the study of plant cells. *Int. Rev. Cytol.* 68:9-51.
- Franke, W. W., E. Seib, W. Herth, M. Osborn, and K. Weber. 1977. Reaction of the anastral mitotic apparatus of endosperm cells of the plant *Leucojum aestivum* with antibodies to tubulin from porcine brain as revealed by immunofluorescence microscopy. *Cell Biol. Int. Rep.* 1:75-83.
- Franke, W. W., E. Seib, M. Osborn, K. Weber, W. Herth, and H. Falk. 1977. Tubulin-containing structures in the anastral mitotic apparatus of endosperm cells of the plant *Leucojum aestivum* as revealed by immunofluorescence microscopy. *Cytobiologie*. 15:24-48.
- Gunning, B. E. S. 1980. Spatial and temporal regulation of nucleating sites for arrays of cortical microtubules in root tip cells of the water fern *Azolla pinnata*. *Eur. J. Cell Biol.* 23:53-65.
- Gunning, B. E. S., and A. R. Hardham. 1979. Microtubules and morphogenesis in plants. *Endeavour (Oxf.)*. 3:112-117.
- Gunning, B. E. S., A. R. Hardham, and J. E. Hughes. 1978. Evidence for initiation of microtubules in discrete regions of the cell cortex in *Azolla* root-tip cells, and an hypothesis on the development of cortical arrays of microtubules. *Planta (Berl.)*. 143:161-180.
- Gunning, B. E. S., J. E. Hughes, and A. R. Hardham. 1978. Formative and proliferative cell division, cell differentiation, and developmental changes in the meristem of *Azolla* roots. *Planta (Berl.)*. 143:121-144.
- Hanzely, L., and O. A. Schjeide. 1973. Structural and functional aspects of the anastral mitotic spindle in *Allium sativum* root tip cells. *Cytobios*. 7:147-162.
- Hardham, A. R., P. B. Green, and J. M. Lang. 1980. Reorganization of cortical microtubules and cellulose deposition during leaf formation in *Gratiopetalum paraguayense*. *Planta (Berl.)*. 149:181-195.
- Hardham, A. R., and B. E. S. Gunning. 1978. Structure of cortical microtubule arrays in plant cells. *J. Cell Biol.* 77:14-34.
- Hepler, P. K. 1976. Plant Microtubules. In *Plant Biochemistry*. J. Bonner and J. E. Varner, editors. Academic Press, Inc., New York. 147-187. 3rd Edition.
- Hepler, P. K. 1981. Morphogenesis of tracheary elements and guard cells. In *Cytomorphogenesis in Plants*. O. Kiermayer, editor. Springer-Verlag, New York/Wien. In press.
- Hepler, P. K., and W. T. Jackson. 1968. Microtubules and early stages of cell-plate formation in the endosperm of *Haemaphys katherinae* Baker. *J. Cell Biol.* 38:437-446.
- Hepler, P. K., and E. H. Newcomb. 1967. Fine structure of cell plate formation in the apical meristem of *Phaseolus* roots. *J. Ultrastruct. Res.* 19:498-513.
- Hepler, P. K., and B. A. Palevitz. 1974. Microtubules and microfilaments. *Annu. Rev. Plant Physiol.* 25:309-362.
- Klein, S., and B. Ginzburg. 1960. An electron microscope investigation into the effect of EDTA on plant cell walls. *J. Biophys. Biochem. Cytol.* 7:335-338.
- Knox, R. B., H. I. M. V. Vithanage, and B. J. Howlett. 1980. Botanical Immunocytochemistry. A review with special reference to pollen antigens and allergens. *Histochem. J.* 12:247-272.
- Latham, D. S. 1960. The separation of plant cells with ethylenediaminetetraacetic acid. *Exp. Cell Res.* 21:353-360.
- Lloyd, C. W., A. R. Slabas, A. J. Powell, and S. B. Lowe. 1980. Microtubules, protoplasts and plant cell shape. An immunofluorescent study. *Planta (Berl.)*. 147:500-506.
- Lloyd, C. W., A. R. Slabas, A. J. Powell, G. MacDonald, and R. A. Badley. 1979. Cytoplasmic microtubules of higher plant cells visualized with anti-tubulin antibodies. *Nature (Lond.)*. 279:239-241.
- Marchant, H. J. 1978. Microtubules associated with the plasma membrane isolated from protoplasts of the green alga *Mougeotia*. *Exp. Cell Res.* 115:25-30.
- Osborn, M., and K. Weber. 1977. The display of microtubules in transformed cells. *Cell*. 12:561-571.
- Pickett-Heaps, J. D., and D. H. Northcote. 1966. Organization of microtubules and endoplasmic reticulum during mitosis and cytokinesis in wheat meristems. *J. Cell Sci.* 1:109-120.
- Pickett-Heaps, J. D., and D. H. Northcote. 1966. Cell division in the formation of the stomatal complex of the young leaves of wheat. *J. Cell Sci.* 1:121-128.
- Powell, A. J., C. W. Lloyd, A. R. Slabas, and D. J. Cove. 1980. Demonstration of the microtubular cytoskeleton of the moss, *Physcomitrella patens*, using antibodies against mammalian brain tubulin. *Plant Sci. Lett.* 18:401-404.
- van der Valk, P., P. J. Rennie, J. A. Connolly, and L. C. Fowke. 1980. Distribution of cortical microtubules in tobacco protoplasts. An immunofluorescence microscopic and ultrastructural study. *Protoplasma*. 105:27-43.
- Weber, K., and M. Osborn. 1979. The intracellular display of microtubular structures revealed by indirect immunofluorescence microscopy. In *Microtubules*. K. Roberts and J. S. Hyams, editors. Academic Press, Inc., New York. 279-313.
- Weber, K., M. Osborn, W. W. Franke, E. Seib, U. Scheer, and W. Herth. 1977. Identification of microtubular structures in diverse plant and animal cells by immunological cross-reaction revealed in immunofluorescence microscopy using antibody against tubulin from porcine brain. *Cytobiologie*. 15:285-302.
- Weber, K., J. Wehland, and W. Herzog. 1976. Griseofulvin interacts with microtubules both *in vivo* and *in vitro*. *J. Mol. Biol.* 102:817-829.